VOL. 15, NO. 3, FEBRUARY 2020 ISSN 1819-6608
ARPN Journal of Engineering and Applied Sciences

www.arpnjournals.com

INVESTIGATION OF STRUCTURAL RESPONSE OF FLOOR PANEL UNIT ON THE PORTABLE BLAST ROOM USING FINITE ELEMENT METHOD

Aulia Windyandari[1], Haryono Setyo Huboyo[2] and Ahmad Fauzan Zakki[3]
[1]Vocational Program of Naval Architecture Department, Engineering Faculty, Diponegoro University, Semarang, Indonesia
[2]Environmental Engineering Department, Engineering Faculty, Diponegoro University, Semarang, Indonesia
[3]Naval Architecture Department, Engineering Faculty, Diponegoro University, Semarang, Indonesia
E-Mail: auliawindyandari@lecturer.undip.ac.id

ABSTRACT

The abrasive blasting and the other surface preparation techniques are the significant sources of shipyard waste and air pollution. The one of any kind techniques to reduce the hazardous air contaminant associated with the abrasive media is blasting room. The abrasive blasting operation is isolated by the blasting room to reduce the exposure to the shipyard environment. The portable blasting room design has been developed using the modular wall panel system. The research is focused on the investigation of structural response of floor panel unit of the portable modular blast room using finite element method. The research method has two main steps during the investigation of the floor panel unit of portable blast room. At first, the geometric form of the floor panel unit was developed and defined to obtain the finite element model. Secondly, the load and boundary condition was defined, considering the cradle load which is carry the blasted object to the blast room. The displacement method was adopted for the numerical analysis. The results indicate that the structure of floor panel unit on the portable modular blast room is safe and reliable for abrasive blasting isolation room.

Keywords: portable blast room, floor panel unit, structural response.

INTRODUCTION

Abrasive blasting is the system of blowing abrasive particles from a blast machine, using the power of compressed air. Three primary components compose a blast equipment setup: air compressor, blast machine, and abrasive. The sufficient air pressure and volume must be produced by the compressor to convey abrasive from the blast machine to the surface being blasted. Air pressure is typically high, at 100 pounds per square inch, and nozzle velocities can approach 650 - 1,700 feet per second, [1]. The lack of one part of the components may reduce the productivity of abrasive blasting system.

In the shipbuilding and ship repair industry, the most common surface preparation technique used to clean production objects such ship hull, parts, components, plates and profiles is abrasive blasting. Abrasive blasting might be conducted in the new building ship production process such as fabrication, sub assembly, assembly, erection and coating/painting. Instead of the new building process, the abrasive blasting also significantly be utilized for maintenance and ship repair activities. The abrasive blasting and the other surface preparation techniques are the significant sources of shipyard waste and air pollution. Therefore the abrasive blasting should be conducted within the blasting room as a control action to the waste and pollution in the shipyard environment. An abrasive blast room is the core to any modern abrasive blast system. Confining the blasting operation to a controlled clean environment enables efficient abrasive recycling.

There have been a number of different reports on the abrasive blast room development for the improvement of abrasive process, work environment and reducing the manufacturing cost. Walter L. Keefer [2] produced the blasting room for cleaning of castings. The invention is applicable to core knockout rooms in which water jet is employed to breakdown and blast away the molding cores used in the founding of large hollow castings, Figure-1. Leroy C. Haker [3] developed a grid-like floor of sand blast room which the abrasive material resulting from sand blasting operations may fall and recycled, Figure-2. Richard E. Lewis [4] produced a tent-like portable blasting room enclosure with a central entry opening in the roof, Figure-3. The blasting room enclosure is mounted on rollers and a track extends parallel with the air return ducts to permit the blasting room enclosure to be moved between the first and second floor areas so that parts to be cleaned can be removed and placed in the open floor area while sandblasting is taking place in the other adjacent floor area.

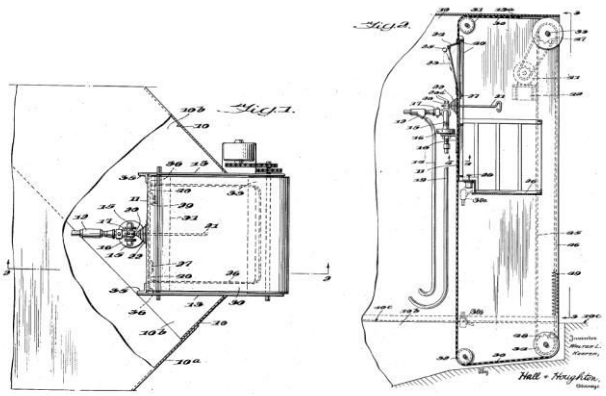

Figure-1. The design of blasting room Walter L Keefer, [2].

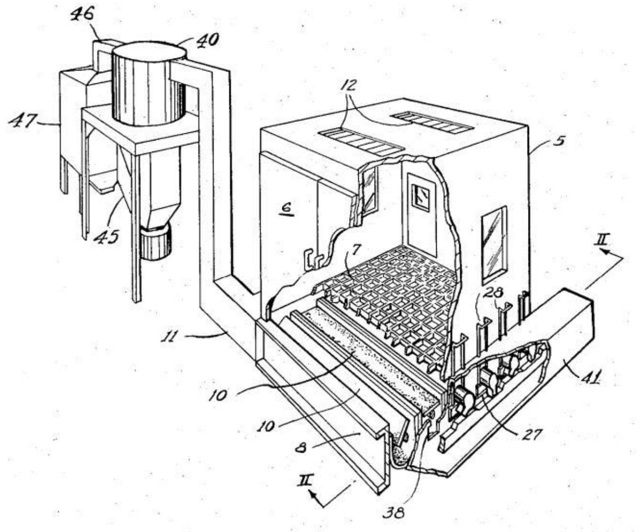

Figure-2. The design of sand blast room by Leroy C. Haker, [3].

Recent development has shown the application of containerized blast room which offer an affordable solution when weatherproofed or transportable blast room is required, Figure-4. Besides standard shipping size, the containerized blast room provides an enclosure built on the principles of a shipping container, but manufacture to any size. The other type of portable blast room is modular blast room. Modular blast rooms are made primarily from a standard 2mm galvanized steel formed panel complemented with heavy duty doors and door frames, Figure-5. It can be built up to almost any shape and size from a 10ft cube to a booth capable of enclosing a rail carriage and beyond.

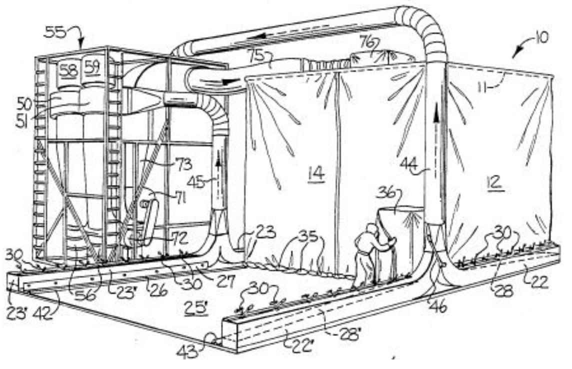

Figure-3. The design of abrasive blasting containment system by Richard E Lewis, [4].

Figure-4. The containerized blast room.

Figure-5. The modular blast room.

The portable blast room that commonly used to support the abrasive cleaning activities usually made from steel and galvanized steel. These metal materials have advantages for the strength of the structures of blast room to withstand the load. However the weight of the steel panel is heavy compared than composites. Since the portable blast room should be compact, light and flexible, therefore the portable blast room using modular composite wall panel (Glass Reinforced Plastic) was developed to improve the flexibility, and to enhance the knockdown system for the erection of the portable blast room, Figure-6.

The needs and requirements for adequate structures of the floor panel unit of modular portable blast room has motivate this research to focus on the investigation of structural strength of the proposed floor panel design, Figure-7. The modular floor panel units were assembled for the portable blast room to support the self-collecting abrasive waste material. The knockdown and modular system was adopted to give the flexibility, adaptability and simplicity for the installation of the portable blast room.

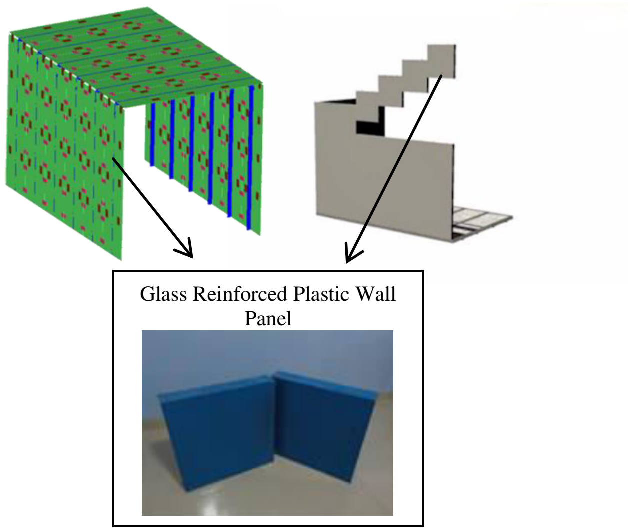

Figure-6. The portable blast room using fiberglass modular wall panel, [5].

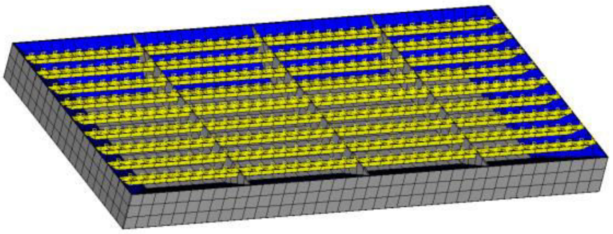

Figure-7. The proposed design of floor panel unit of the portable blast room.

MATERIALS AND METHODS

In designing the work floor of portable blast room, knockdown assembly system is also used for the erection process. Work floor was designed using panel unit that can be assembled and arranged to obtain the desired work floor area. In addition to the use of knockdown system, several other considerations that are used in the process of designing the work floor is the strength of floor construction, as well as their compartment or a place to collect particle or waste material on the work floor. Based on these considerations, the design dimension of the floor panel units are developed as follow:

1. Length (L)	:	2 m
2. Width (B)	:	1 m
3. Height (H)	:	1.5 m

The research method has two main steps during the structure analysis of floor panel unit for portable blasting room. At first, the geometric form of modular floor panel units was developed and defined to obtain the finite element model. The displacement method was adopted for the numerical analysis. Secondly, the load and boundary condition was defined, considering the cradle and the blasted object weight load which are exerted to the floor panel unit structure as a concentrated load.

Finite element formulations for Mindlin plates

Since computers is adopted as hardware to support the design and engineering activities, nowadays, finite element analysis are widely implemented in the marine and other manufacture industries. The flexibility and versatility is offered by finite element analysis to solve the complex engineering problems. FEA can be used to analyze the strength of marine structure such as ship, submarine pressure hull, floating pontoon, free-fall lifeboat and floating cage, [6-12]

The present study deals with shell elements that are obtained as the Mindlin-Reissner plate elements. The Mindlin plate theory is considered as an extension of the Timoshenko beams theory in bending. The formulation has been carried out employing the four-noded plates. The Mindlin plate theory or first-order shear deformation theory for plates includes the effect of transverse shear deformations. The main difference with Kirchhoff-type theories is that in the Mindlin theory the normals to the undeformed middle plane of the plate remain straight, but not normal to the deformed middle surface.

The strain energy of the Mindlin plate is given as:

$$U = \frac{1}{2}\int_V \sigma_f^T \epsilon_f \, dV + \frac{\alpha}{2}\int_V \sigma_c^T \epsilon_c \, dV \tag{1}$$

where,

$$\sigma_f^T = [\sigma_x \quad \sigma_y \quad \tau_{xy}] \tag{2}$$

$$\epsilon_f^T = [\epsilon_x \quad \epsilon_y \quad \gamma_{xy}] \tag{3}$$

are the bending stress and strains, and

$$\sigma_c^T = [\tau_{xz} \quad \tau_{yz}] \tag{4}$$

$$\epsilon_c^T = [\gamma_{xz} \quad \gamma_{yz}] \tag{5}$$

are the transverse shear stresses and strains. The α parameter, is known as the shear correction factor commonly be given as 5/6, [6]. The displacement field for plate with thickness h is defined as

$$u = z\theta_x \; v = z\theta_y \; w = w_0 \tag{6}$$

where θ_x and θ_y are the rotations of the normal to the middle plane with respect to axes *y* and *x*, respectively. Bending strains are taken as

$$\epsilon_x = \frac{\partial u}{\partial x} = z\frac{\partial \theta_x}{\partial x} \tag{7}$$

$$\epsilon_y = \frac{\partial v}{\partial y} = z\frac{\partial \theta_y}{\partial x} \tag{8}$$

$$\gamma_{xy} = \frac{\partial u}{\partial y} + \frac{\partial v}{\partial x} = z\left(\frac{\partial \theta_y}{\partial x} + \frac{\partial \theta_x}{\partial y}\right) \tag{9}$$

and the transverse shear deformations are given as

$$\gamma_{xz} = \frac{\partial w}{\partial x} + \frac{\partial u}{\partial z} = \frac{\partial w}{\partial x} + \theta_x \tag{10}$$

$$\gamma_{yz} = \frac{\partial w}{\partial y} + \frac{\partial v}{\partial z} = \frac{\partial w}{\partial y} + \theta_y \tag{11}$$

The linear elastic stress-strain relations in bending are defined for a homogeneous, isotropic material as

$$\sigma_f = \mathrm{D_f}\epsilon_f \tag{12}$$

where $\mathrm{D_f}$ is defined as

$$\mathrm{D_f} = \frac{\mathrm{E}}{1-\nu^2}\begin{bmatrix} 1 & \nu & 0 \\ \nu & 1 & 0 \\ 0 & 0 & \frac{1-\nu}{2} \end{bmatrix} \tag{13}$$

while the linear elastic stress-strain relations in transverse shear are defined as

$$\sigma_c = \mathrm{D_c}\epsilon_c \tag{14}$$

where

$$\mathrm{D_c} = \begin{bmatrix} G & 0 \\ 0 & G \end{bmatrix} \tag{15}$$

where $G$the shear modulus. Introducing these concepts into the strain energy, the formulation is obtained as

$$U = \frac{1}{2}\int_V \epsilon^T D_f \epsilon_f \, dV + \frac{\alpha}{2}\int_V \epsilon_c^T D_c \epsilon_c \, \mathrm{dV} \tag{16}$$

The generalized displacements are independently interpolated using the same shape functions

$$\mathrm{w} = \sum_{i=1}^{n} \mathrm{N_i}(\xi,\eta)\mathrm{w_i} \; \theta_\mathrm{x} = \sum_{i=1}^{n} \mathrm{N_i}(\xi,\eta)\theta_{\mathrm{xi}}$$

$$\theta_\mathrm{y} = \sum_{i=1}^{n} \mathrm{N_i}(\xi,\eta)\theta_{\mathrm{yi}}$$

where $N_i(\xi,\eta)$ are the shape functions of a bilinear four-noded Q4 element.
Strains are defined as

$$\epsilon_f = z\mathrm{B}_f\mathrm{d}^e; \; \epsilon_c = \mathrm{B}_c\mathrm{d}^e \tag{17}$$

The corresponding strain-displacement matrices B are described as follow.
the bending component

$$\mathrm{B_f^{(e)}} = \begin{bmatrix} 0 & \frac{\partial N_1}{\partial x} & 0 & \cdots & 0 & \frac{\partial N_2}{\partial x} & 0 \\ 0 & 0 & \frac{\partial N_1}{\partial y} & \cdots & 0 & 0 & \frac{\partial N_2}{\partial y} \\ 0 & \frac{\partial N_1}{\partial y} & \frac{\partial N_1}{\partial x} & \cdots & 0 & \frac{\partial N_2}{\partial y} & \frac{\partial N_2}{\partial x} \end{bmatrix} \tag{18}$$

and the shear component

$$\mathrm{B_c^{(e)}} = \begin{bmatrix} \frac{\partial N_1}{\partial x} & N_1 & 0 & \cdots & \frac{\partial N_2}{\partial x} & N_2 & 0 \\ \frac{\partial N_1}{\partial y} & 0 & N_1 & \cdots & \frac{\partial N_2}{\partial y} & 0 & N_2 \end{bmatrix} \tag{19}$$

where

$$\mathrm{d^{eT}} = \{\mathrm{w_1} \quad \theta_{\mathrm{x1}} \quad \theta_{\mathrm{y1}} \quad \ldots \quad \mathrm{w_4} \quad \theta_{\mathrm{x4}} \quad \theta_{\mathrm{y4}}\} \tag{20}$$

The plate strain energy is obtained as

$$U = \frac{1}{2}\mathrm{d}^{eT}\int_{\Omega^e}\int_z \mathrm{B_f^T}\mathrm{D_f}\mathrm{B}_f \, dz d\Omega^e \mathrm{d^e} + \frac{\alpha}{2}\mathrm{d^{eT}}\int_{\Omega^e}\int_z \mathrm{B_c^T D_c B_c dz d\Omega^e d^e} \tag{21}$$

The stiffness matrix of Mindlin plate is then obtained as

$$\mathrm{K^e} = \frac{\mathrm{h^3}}{12}\int_{\Omega^e} \mathrm{B_f^T D_f B_f d\Omega^e} + \alpha\mathrm{h}\int_{\Omega^e} \mathrm{B_c^T D_c B_c d\Omega^e} \tag{22}$$

or

$$\mathrm{K^e} = \frac{\mathrm{h^3}}{12}\int_{-1}^{1} \mathrm{B_f^T D_f B_f |J| d\xi d\eta} + \alpha\mathrm{h}\int_{-1}^{1} \mathrm{B_c^T D_c B_c |J| d\xi d\eta} \tag{23}$$

where $|J|$is the determinant of the Jacobian matrix

The vector of nodal forces equivalent to distributed forces P is defined as

$$\mathrm{f^e} = \int_{-1}^{1}\int_{-1}^{1} \mathrm{N \; P \; |J| \; d\xi d\eta} \tag{24}$$

Both the stiffness matrix and the force vector integrals are computed by numerical integration. The stiffness integral is solved by considering for the Q4 element, 2×2 Gauss points for the bending contribution and 1 point for the shear contribution. This selective integration proved to be one of the simplest remedies for avoiding shear locking [13, 14].

Cradle load and boundary condition

In the process of blasting, the object is placed on the cradle that equipped with the wheels that can be drawn into portable blast room. The load which is act to the floor panel structure is induced by the force on the wheel cradle. The maximum weight of the blasted object is determined by the weight of one sheet plates with the thickness of 10 mm, the length of 6000 mm and the width of 1800 mm. Furthermore, from the weight of blasted object include with the weight of the cradle, the total force was divided by the total number of wheels that support the load. Therefore the concentrated load of the floor panel unit structure was obtained as -0.03532 MN.

Through the design geometry that had been obtained, furthermore the floor panel unit structure was determined to withstand the given load. The floor panel structure was designed as a compartment with grating shaped on the topside deck that was intended to collect the waste materials. Additionally, the bolted clevis was adopted for the connection system between the panel units. Prior to supporting sandblasting process, an evaluation of the portable blasting room strength must be established and confirmed. The estimation of structural response behavior due to operational loads is important for a reliable design. The strength assessment of portable blasting room was focused on the investigation of the strength of floor panel unit structure using finite element method. The finite element (FE) model was developed for the floor panel unit strength analysis. The requirements that should be followed by the developed FE model are:

- All main structural members are to be presented in the FE model
- Grid like topside deck are to be modeled by beam element having axial and bending stiffness
- Floor panels are to be modeled by shell element having out-of-plane bending stiffness in addition to bi-axial and in-plane stiffness

Table-1. Support conditions of the boundary point.

Location of the boundary point	**Translational**		
	Dx	**Dy**	**Dz**
The boundary point on the bottom of floor panel	Fix	Fix	Fix
Location of the boundary point	Rotational		
	Rx	Ry	Rz
The boundary point on the bottom of floor panel	Fix	Fix	Fix

Table-2. Material properties of steel.

Typical Properties	**Steel**
Density (Ton/mm^3)	7.83×10^{-9}
Young Modulus (MPa)	2.07×10^5
Poisson Ratio	0.30
Yield Strength (MPa)	2.35×10^3

Boundary conditions have been defined as simply supported at the bottom floor of the FE model. The nodes on the floor panel at the bottom side of the portable blasting room are to be fixed as presented in the Table-1. The material properties was defined as the properties of steel, see Table-2. The loading conditions were used in the analysis including the cradle load and the blasted object weight load. The illustrations of the FE model, boundary and the loading conditions are described in the Figure-8.

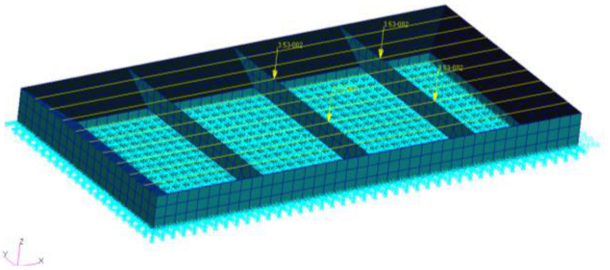

Figure-8. The load and boundary condition of the floor panel unit.

RESULTS AND DISCUSSIONS

The FE model that has been defined with the loading and boundary condition was analyzed using finite element method. The linear static analysis was chosen to solve the problem case. The structure of the floor panel unit was modeled using 1826 shell elements and 360 beam elements. The shell elements were mixed using quadrilateral and triangular elements. Computing time required for the analysis is 1.2 minutes on an AMD V120 Processor 2.2 GHz with 2 GB RAM running Windows 7. The illustration of the results of numerical analysis might be seen in Figures 9-13.

The results of the numerical analysis are Von Mises stress plots on the finite elements for particular parts of the structure. The stress results presented correspond to the layer that exhibits the highest stress. The deformation of the FE model was exaggerated for visualization purposes.

In general, it may be seen that the boundary conditions perform quite well, as there is no visible effect on the stress field. At the wall panel the stress distribution is uniform and not affected by the boundary conditions. The nodes which constraint was defined also have shown no stress concentration.

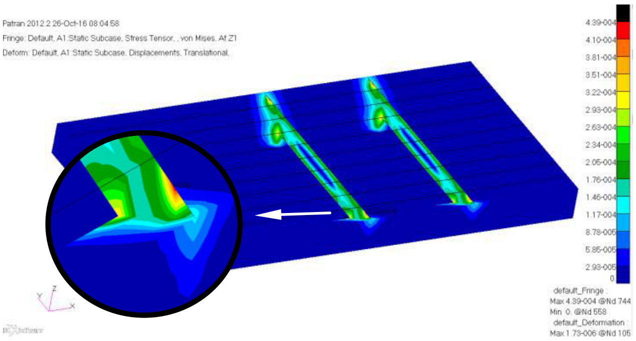

Figure-9. The stress distributions on the floor panel unit of the portable blast room

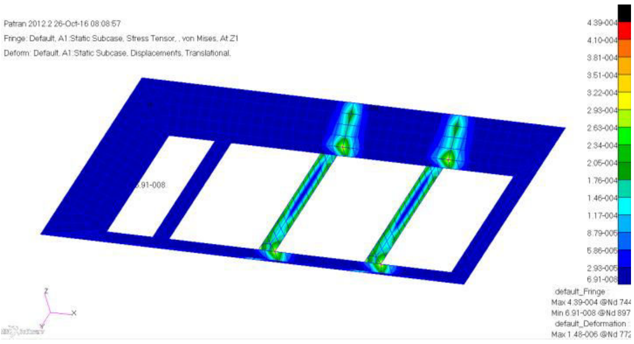

Figure-10. The stress distributions on the topside of the floor panel unit.

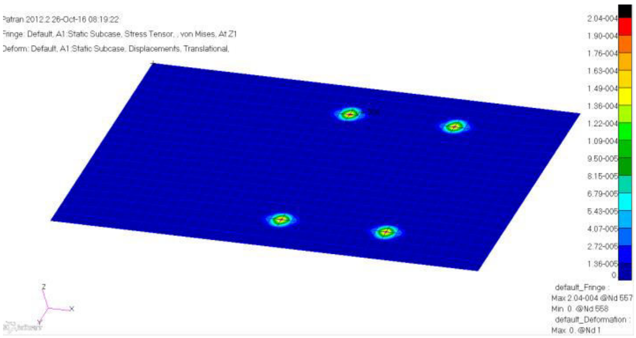

Figure-11. The stress distributions on the bottom side of the floor panel unit.

In Figures 9-10, the maximum stress of the topside part of the floor panel unit was occurred at the web girder of the topside part of the floor panel unit. It can be explained that the stress was induced by the concentration force which is generated by the load on the wheel of the cradle. These stresses are about 4.39 × 10^{-4} MPa, significantly smaller than the permissible stress (175 MPa). The maximum stress of the bottom side of the floor panel unit, in Figure-11 is about 2.04 × 10^{-4} MPa which was occurred at the below of web girder. It may be explained that the concentrated load was distributed by web girder to the bottom part of the floor panel unit. Therefore, the stress concentration was appeared in the bottom at the adjacent part where the concentrated load was located.

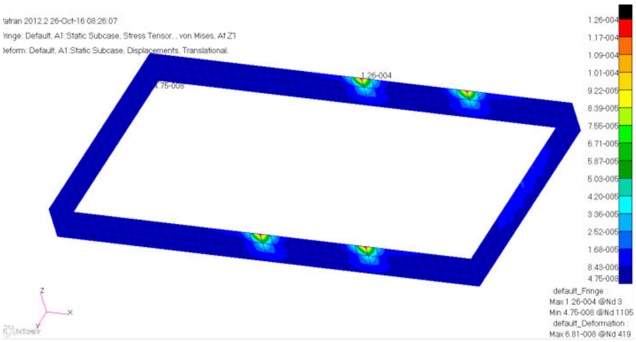

Figure-12. The stress distributions on the wall side of the floor panel unit.

Figure-13. The stress distributions on the grid of the floor panel unit.

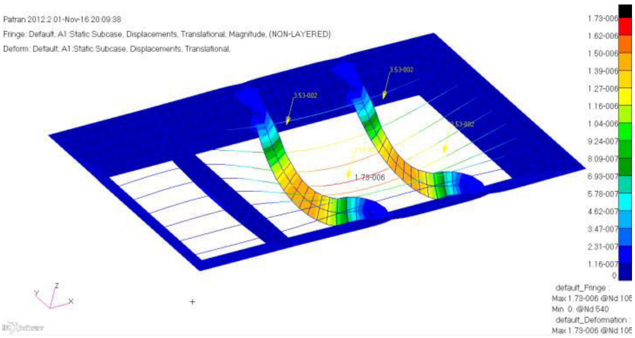

Figure-14. The displacement of the floor panel unit.

In the wall side of the floor panel, it is shows that the maximum stress is located at the similar region of the maximum stress on the topside of the floor panel, the stresses is about 1.26×10^{-4}MPa. However it is significantly smaller than the stress at the topside of the floor panel, in Figure-12. It is indicated that the maximum stress on the wall side was induced by the stress concentration on the web girder as the topside part. Finally, the grid of the floor panel, Figure-13 shows that the maximum stresses are about 1.75×10^{-4}MPa, which is located at the connection joint of unloaded web girder and the beam (grid) structure. As expected, the results of the strength analysis show that the structure of the floor panel unit is reliable to support the cradle and the blasted object load on the portable blasting room. The maximum stress was occurred at the web girder of the floor panels below the permissible stress (175 MPa) with the maximum displacement is 1.73×10^{-6}mm, in Figure-14. Regarding the maximum stresses and displacement, it might be determined that the structures of the floor panel unit of the portable modular blast room are safe and reliable for supporting the abrasive blasting process as an isolation room.

CONCLUSIONS

An investigation of structural response of the floor panel unit on the portable blast room to support abrasive blasting process was made, utilizing the simulation and numerical analysis.

The evaluation of the floor panel unit strength was calculated using finite element method comprising, to build FE model (meshing), to define the load and boundary conditions, to define the material properties and structure scantlings.

The cradle and blasted object weight was selected for the load of the strength analysis. Hence, the maximum stress of4.39×10^{-4}MPa which was occurred at the web girder of the floor panel unit, significantly smaller than the permissible stress (175 MPa). It is concluded that the structure of floor panel unit on the portable modular blast room is safe and reliable for abrasive blasting isolation room.

REFERENCES

[1] OSHA. 2006. Abrasive Blasting Hazards in Shipyard Employment. An OSHA Guidance Document, U.S. Department of Labor Occupational Safety and Health Administration Directorate of Standards and Guidance Office of Maritime

[2] W. L. Keefer. 1948. Blasting Room. United States Patent Office, Application March 2, 1946, Serial No. 651, 641.

[3] C. L. Haker. 1975. Sand blast room. United States Patent Office, Patent Number: 3863392, Date of patent: Feb. 4, 1975.

[4] R. E., Lewis. 1987. Abrasive blasting containment system. United States Patent Office, Patent Number: 4787179, Date of patent: Nov. 29, 1988.

[5] A. Windyandari, S. D. Said, and A. F. Zakki. 2015. The development of portable blast room to reduce the air polution in shipyard environtment. Final reports of the Competitive Research Grant (Hibah Bersaing), Nopember.

[6] F. Zakki, A. Windyandari and D. M. Bae. 2016. The development of new type free-fall lifeboat using Fluid Structure Interaction analysis. Journal of Marine Science and Technology (Taiwan). 24: 575-580.

[7] Windyandari, S. D. Said and A. F. Zakki. 2017. Strength Analysis of Portable Blast Room Using Modular GlassReinforced Plastics Wall Panel by Finite Element Method. Applied Mechanics Materials. 862: 302-307.

[8] Windyandari H. Yudo and A. F. Zakki. 2017. Comparative studies on buckling strength between the swedge-stiffened and the ring-stiffened of the midget type submarine pressure hull. ARPN Journal of Engineering and Applied Science. 13: 2340-2346.

[9] H. Yudo, A. Windyandari and A. F. Zakki. 2017. Numerical investigation of the buckling strength behavior of ring stiffened submarine pressure hull. International Journal of Civil Engineering and Technology. 8: 408-415.

[10] A. Windyandari and A. F. Zakki. 2018. The Structural Response Investigation of Modular Pontoon Collar Floating Cage due to Current Load to Support Fish Farming Activities . Matec web of conferences. 159: 01-06.

[11] F. Zakki, A. Windyandari, Q. T. Medina, I. A. C. Abar. 2019. Evaluation of drop test performance of glass fiber reinforced plastic (GFRP) modular pontoon unit using numerical analysis. Journal of Mechanical Engineering Ressearch and Developments. 42: 106-110.

[12] R. Prabowo, D. M. Bae, J. M., Sohn, B. Cao, and Q. Wang. 2018. Analysis of structural damage on the struck ship under side collision scenario. Alexandria Engineering Journal. 57: 1761-1771.

[13] Reddy J. N. 1993. An introduction to the finite element method. McGraw-Hill, New York.

[14] K. J. Bathe. 1982. Finite element procedures in engineering analysis. Prentice-Hall, Englewood Cliffs, NJ.